Desalination and Water Treatment
www.deswater.com
49 (2012) 337–347
November
1944-3994/1944-3986
doi: 10.1080/19443994.2012.719363
Taylor & Francis
Taylor & Francis Group

Novel removal of water-insoluble disperse dye onto a low-cost adsorbent prepared from tropical fruit waste

Siti Hazirah Adam[a], Aishah Abdul Jalil[a,*], Sugeng Triwahyono[b]

[a]*Institute of Hydrogen Economy, Faculty of Chemical Engineering, Universiti Teknologi Malaysia, 81310 UTM Johor Bahru, Johor, Malaysia*
Tel. +60 7 5535581; Fax: +60 7 5536165; email: aishah@cheme.utm.my
[b]*Nanotechnology Research Alliance, Universiti Teknologi Malaysia, 81310 UTM Johor Bahru, Johor, Malaysia*

Received 8 August 2011; Accepted 15 July 2012

ABSTRACT

The potential of tropical fruit waste (*durio zibethinus* husk, DZH) as a low-cost adsorbent for removal of disperse blue 60 (DB 60) from an aqueous medium was studied under various conditions such as effects of adsorbent surface modification, contact time, pH, and temperature. The removal percentage of DB 60 was enhanced by approximately a factor of six when using the DZH treated by mineral acid compared to the untreated DZH. The functional groups of DZH before and after acid treatment were analyzed by Fourier transform infrared spectroscopy to elucidate these results. The surface structure of the DZH before and after adsorption was analyzed by field emission scanning electron microscopy. Adsorption equilibrium isotherms and kinetics of the DZH were studied using Langmuir and Freundlich models, as well as pseudo-first-order, second-order kinetic and intraparticle diffusion equations. The Langmuir isotherm model agreed well with the experimental data with a maximum adsorption capacity (q_{max}) of 54.6 mg g^{-1}. The data followed the pseudo-second-order equation. Thermodynamic studies showed that the adsorption was endothermic and not spontaneous at low temperature, and was controlled by a chemisorption process. The results show that DZH could be used as a low-cost material to compare with activated carbon for the removal of disperses dyes from effluents.

Keywords: Adsorption; Disperse blue dye; Tropical fruit waste; *durio zibethinus*; Isotherm; Kinetic

1. Introduction

Disperse dyes are widely used in a variety of industries, such as textile, paper and leather. Generally recognized as non-ionic aromatic compounds, they have low solubilities in water, but are highly soluble in organic solvents. The effluents of these industries may produce harmful effects on the health of living organisms and the environment if not treated properly before being discharged into bodies of water. The effluents can affect aesthetic qualities and interfere with the transmission of sunlight in streams, which can reduce photosynthetic activity [1]. Therefore, the treatment of such industrial dye effluents is of great interest to decrease the concentrations of the dyes as required under environmental regulation acts [2–4].

A number of low-cost alternative adsorbents have been explored for the removal of disperse dyes but the adsorption capacity is not very large; to improve adsorption performance new adsorbents are still

*Corresponding author.

under development. *Durian* is a well-known and well-liked fruit in Malaysia that is cultivated in many areas and is produced throughout the year. Due to the high consumption of the fruit, massive amounts of its wastes are disposed, which creates foul odors that attract insects. For this reason, discovering uses for its waste, especially on a large scale, would be beneficial from an environmental and economical point of view. It has been reported that *durio zibethinus* husk (DZH) largely consists of holocellulose, α-cellulose, lignin, and hemi-cellulose [5]. These characteristics make it attractive as an adsorbent for the removal of heavy metal ions. We recently reported on the ability of DZH to efficiently recover gold(III) ions from aqueous solution [6]. However, there is scarce data available on water-insoluble disperse dye removal using this abundant tropical fruit waste. Therefore, this study attempts to determine the potential of the DZH as an alternative low-cost adsorbent system for the removal of Dispersed Blue 60 (DB 60) from aqueous solutions. Fourier transform infrared spectroscopy (FTIR) was used to elucidate the functional groups and field emission scanning electron microscopy (FESEM) to analyze the surface structure of the DZH before and after the adsorption. The equilibrium, kinetics, and thermodynamics of the adsorption are also discussed in detail.

2. Material and methods

2.1. Materials

The species of durian used in this work is *durio zibethinus*, which was collected from a local market. The Dispersed Blue 60 ($C_{20}H_{17}N_3O_5$; molecular weight 379.37, Fig. 1) was obtained from the local textile industry (Ramatex Bhd.) and was used in the condition it was received. The dye solution was prepared to the desired concentration using Milli-Q water.

2.2. Preparation of adsorbent

DZH was cut into small pieces to obtain a suitable size for blending, washed with water to remove any adhering substances, and oven-dried at 100°C. The pieces were then ground to 60-mesh size and oven dried at 100°C for 24 h to constant weight before storing in a plastic bottle. Once in the bottle, the DZH was ready to be used.

Treated DZH was prepared by suspending 2 g of powdered DZH in 200 mL of 1.0 M HCl solution. The mixture was stirred for 4 h at room temperature and then filtered. The resulting adsorbent sample was washed with deionized water several times and oven dried overnight at 100°C.

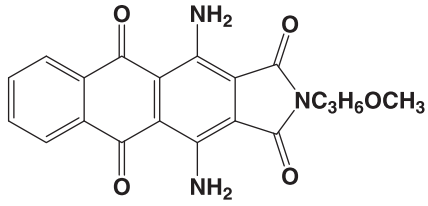

Fig. 1. Dispersed Blue 60.

2.3. Characterization of DZH

Infrared spectra of the DZH samples were obtained using a Fourier transform infrared spectrometer (Spectrum GX, Perkin Elmer, USA). The samples were prepared as KBr pellets and recorded within the range of 400–4,000 cm^{-1} to identify the functional groups that were responsible for adsorption. The morphological features and surface characteristics of the samples were obtained from FESEM using a JEOUL JSM-6701F (Japan) scanning electron microscope at an accelerating voltage of 15 kV. The samples were coated with platinum by electro-deposition under vacuum prior to analyses.

2.4. Adsorption experiments

A stock solution of DB 60 was prepared by dissolving a precise quantity of DB 60 in deionized water and acetone (80/20, v/v). The stock solution was then properly wrapped with aluminum foil and stored in a dark place to prevent direct sunlight, which may cause decolorization. Other required concentrations (10–200 mg L^{-1}) were prepared by diluting the stock solution of DB 60. The pH values of the working solutions were adjusted to the desired values with 0.1 M HCl or 0.1 M NaOH.

Adsorption studies were conducted in 250 mL conical flasks containing 100 mL of dye solution with 1.0 g of DZH. The mixtures were incubated with a stirring rate of 300 rpm at room temperature (30°C) and an initial pH of 9 for 2 h of contact time, which is sufficient to reach equilibrium. Samples were withdrawn at appropriate time intervals and centrifuged at 3,000 rpm for 10 min, and the amount of dye adsorbed was determined using a UV–vis spectrophotometer (Perkin-Elmer, Model Lambda 900, USA) at 585 nm. At any time, the adsorption capacity of dye adsorbed (q_t, mg g^{-1}) onto DZH was calculated using the following mass balance equation:

$$q_t = \frac{(C_0 - C_t)V}{W} \quad (1)$$

where C_0 and C_t (mg L^{-1}) are the liquid-phase concentrations of dye at time zero and at time t, respectively. V (L) is the volume of the solution and W (g) is the mass of DZH used. The dye removal percentage can be calculated as follows:

$$\text{Removal } (\%) = \left(\frac{C_0 - C_t}{C_0}\right) \times 100 \quad (2)$$

3. Results and discussion

3.1. Effect of adsorbent surface modification

The efficiency of raw DZH on the removal of DB 60 from aqueous solutions was tested, and the results are shown in Fig. 2. Only 15% of the DB 60 were removed from the solution when raw (untreated) DZH was used. Therefore, further modification of the DZH was carried out to enhance the electropositivity of the adsorbent surface. The DZH was treated with HCl prior to adsorption. A significant enhancement was observed from which 95% of the maximum removal percentage of DB 60 was achieved after 2 h of adsorption when using the treated DZH. The removal percentage was increased by about six times compared to the adsorption using the untreated DZH. This was likely due to the increase of positively charged cellulose on the surface of DZH following the modification, which provided more attraction sites for the DB 60 anions. This hypothesis was supported by FTIR spectra of treated DZH, shown in Fig. 3, which was compared with spectra from untreated DZH for the three main absorbance regions. Some peaks clearly changed in intensity and shifted after the surface modification, suggesting the participation of certain functional groups of the lignocellulosic material upon treatment. At higher absorbance wavelengths (Fig. 3 (a)), the intensity of a strong band at 3,371 cm^{-1}, which could be attributed to the inter/intrahydrogen bonded (O–H) stretching absorption, was decreased and shifted to 3,368 cm^{-1} [7]. This may be due to the destruction of the hydrogen bonds between the lignin and carbohydrate and also between the cellulosic chains [8]. Both of the adsorption bands at 2,368 cm^{-1}, which can be assigned to the C=O stretching in ketene and 1,740 cm^{-1}, C=O stretching in esters, aldehydes, ketones, and acetyl derivatives, were shifted to 2,340 and 1,728 cm^{-1}, respectively, after the hydrolysis [9]. The strong band at 1,615 cm^{-1} (Fig. 3(b)) in the spectrum of untreated DZH was slightly shifted to higher wavenumbers in the treated DZH spectrum and appeared as a weak band at 1,640 cm^{-1}. This may be ascribed to a deformation occurring in the aryl groups that were originally present as C=C stretching in the untreated DZH to form C–C in-plane bending as a consequence of the HCl treatment [10]. The HCl treatment also changed the relative intensities of the peaks at lower regions (Fig. 3(c)). The increase in intensity of the peak at 1,370 cm^{-1}, which could correspond to –CH bending vibrations, may be due to the introduction of $–CH_2$, $–CH_3$, and –CH groups to the DZH surface [11,12]. The peaks in the range of 1,000–1,250 cm^{-1} were also increased after the acidic treatment, which may imply a relative increase in single-bonded oxygen functional groups, such as phenols, esters, ethers, and lactones [13].

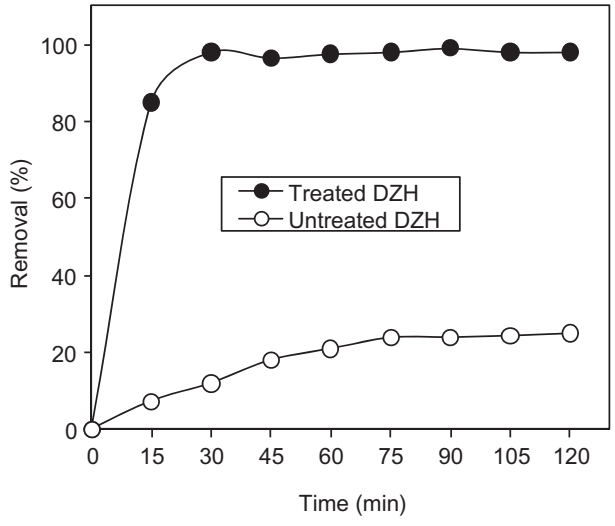

Fig. 2. Effect of DZH surface modification on DB 60 adsorption ($T = 30$ °C, pH = 9, $C_0 = 50$ mg L^{-1}, and $W = 5$ g L^{-1}).

3.2. Effect of initial pH

The pH of aqueous solutions is an important controlling parameter in the adsorption of textile dyes. Fig. 4 illustrates the effect of initial pH on the removal of DB 60 by treated DZH over the pH range of 2–11. The pH did not seem to affect the removal percentage significantly, and DB 60 was almost completely removed from the aqueous solution when the adsorption was carried out between pH 2 and 9. It is well known that imides (DB 60) is to be very stable under acidic conditions, no such electrical repulsion exists, and thus the packing density on the surface of the adsorbent was higher [14,15]. In contrast, the imide is easily hydrolyzed under neutral to alkaline conditions,

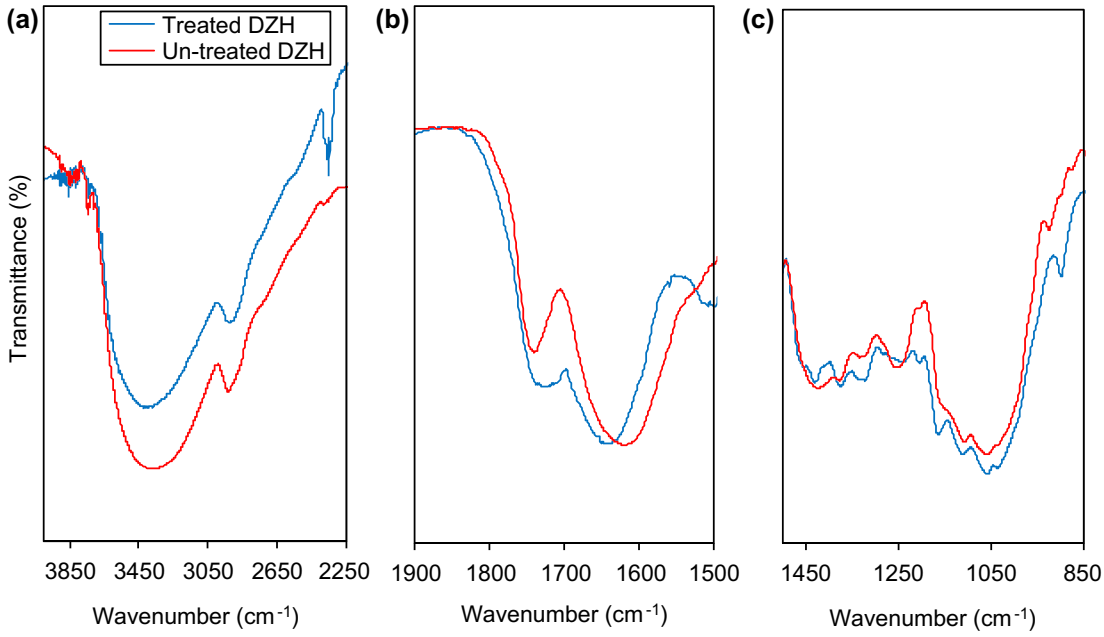

Fig. 3. FTIR spectra of DZH surface before and after treatment by HCl.

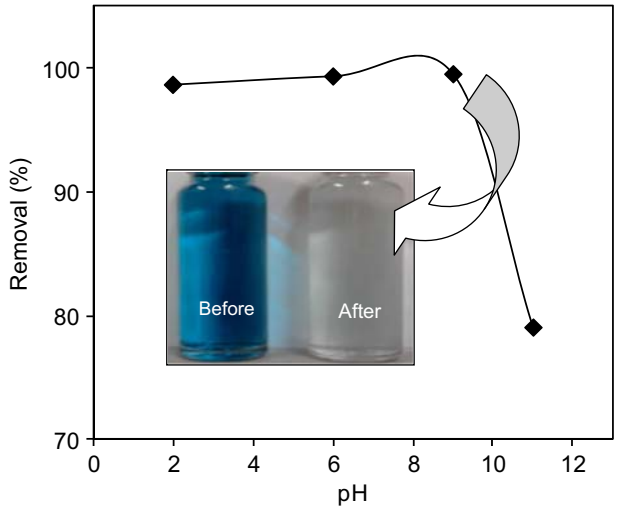

Fig. 4. Effect of pH on the removal of DB 60 onto treated DZH and color change of DB 60 before and after the adsorption ($T = 30$ °C, $W = 2.5\,g\,L^{-1}$, $C_0 = 50\,mg\,L^{-1}$, and time = 120 min).

which lead to the formation of resonance stabilized nitrogen anion flanked by two carbonyls, with the negative charge being distributed over the 5 atoms. Therefore, these anions would bind to the protonated sites ($-OH_2^+$) on the surface of the treated DZH and resulted in a higher removal percentage. However, under strong basic conditions, electrostatic repulsions between the DB 60 anions and abundant hydroxyl ions impeded the adsorption process. Thus, pH 9 was chosen as the appropriate condition in this study because the actual local textile wastewater is weakly alkaline. The color change of $50\,mg\,L^{-1}$ DB 60 at pH 9 is also shown in Fig. 4. The blue color before adsorption became colorless after 120 min of adsorption, verifying that DZH could be used as a potential low-cost absorbent in removing DB 60.

3.3. Effect of adsorbent mass

The effect of treated DZH dosage on the adsorption of DB 60 was investigated in the range of 0.1–1.0 g DZH at room temperature, pH 9, and initial dye concentrations of $50\,mg\,L^{-1}$. It was observed from Fig. 5 that the removal percentage were relatively high in the range of dosage studied, but there was no significant increase in removal when >0.3 g DZH was used. Additionally, 97% of the maximum removal percentage was achieved when 1.0 g of DZH was used. However, the amount of DB 60 adsorbed per unit mass of DZH decreased considerably as the adsorbent dosage increased. A higher dose of absorbent used resulted in more adsorption sites. This led to a higher removal percentage of DB 60, but at the same time resulted in a decrease in adsorption capacity (q).

3.4. Adsorption isotherms

Fig. 6 shows the dependence of the adsorbed amount of DB 60 on equilibrium concentrations in

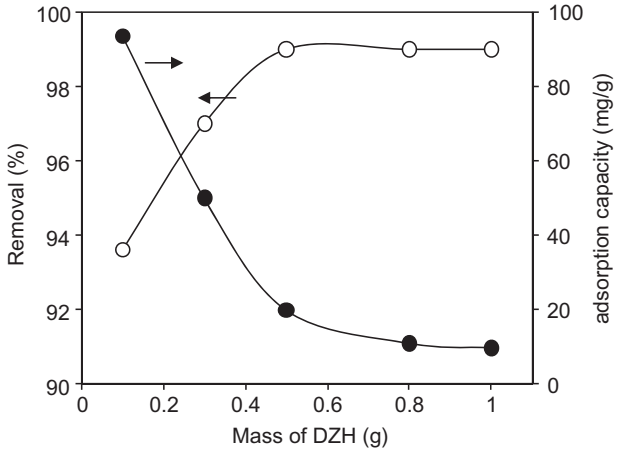

Fig. 5. Effect of adsorbent dosage on the removal (○) and adsorption (●) of DB 60 ($T = 30$ ℃, pH = 9, $V = 0.2$ L, and $C_0 = 50$ mg L^{-1}).

solution at 30℃. The adsorption capacity of DB 60 increased with increasing solution concentration (Fig. 6(a)), and the curves of q_e vs. C_e were "L-shaped" (Fig. 6(b)) according to the classification of Giles et al. [16]. This was a Langmuir-type isotherm, suggesting that there was no strong competition between the solvent and the adsorbate to occupy the adsorbent surface sites, that is, there was a strong preferential adsorption of DB 60 [17].

Next, the adsorption isotherms of DB 60 were interpreted using the well-known Langmuir [18] and Freundlich [19] equation models to understand the extent and degree of favorability of adsorption. The Langmuir isotherm model signifies a monolayer adsorption. It indicates the surface homogeneity of adsorbent and hints towards the conclusion that the adsorbent surface is composed of small adsorption patches that are energetically equivalent to each other with respect to adsorption phenomena [20]. The Langmuir equation is given by:

$$\frac{1}{q_e} = \frac{1}{K_L q_m C_e} + \frac{1}{q_m} \tag{3}$$

where C_e is the concentration of dye solution at equilibrium (mg L^{-1}), q_e and q_m are the equilibrium and maximum amount of dye adsorbed per specified amount of adsorbent at equilibrium (mg g^{-1}), respectively, and K_L is the Langmuir equilibrium constant, which is related to the energy of adsorption. The Langmuir constants K_L and q_m can be determined from the intercept and slope, respectively, of the linear plot of $1/q_e$ vs. $1/C_e$ (Fig. 7(a)) and are presented in Table 1. A further analysis of the Langmuir

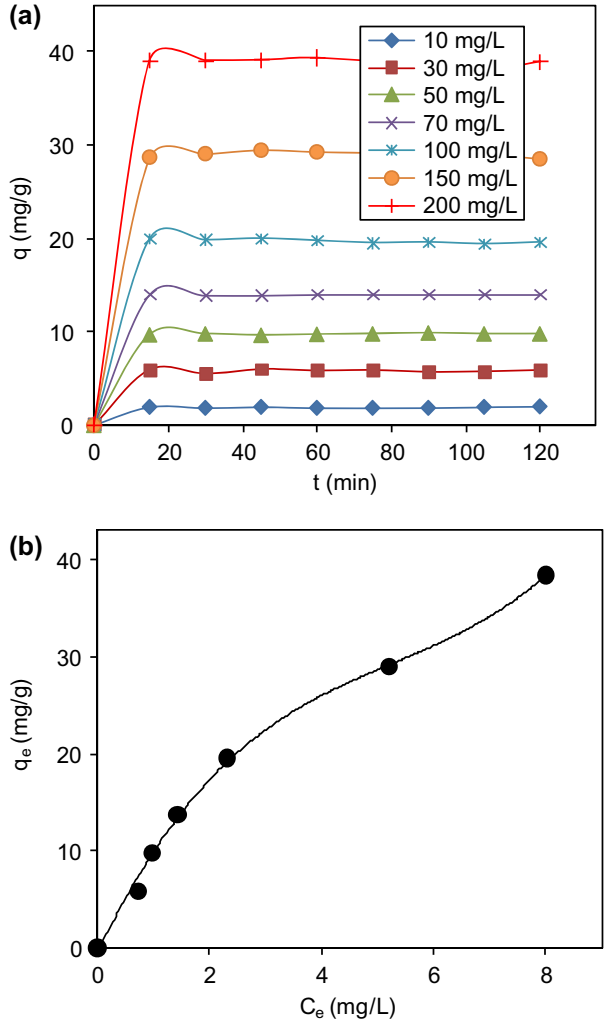

Fig. 6. Effect of equilibrium dye concentration on the adsorption of DB 60 by treated DZH (a) and adsorption isotherm of DB 60 onto treated DZH (b) ($T = 30$ ℃, pH 9, $W = 5$ g L^{-1}, and $t = 120$ min).

isotherm can be made on the basis of a dimensionless equilibrium parameter, R_L [12], also known as the separation factor, which is given by Eq. (4):

$$R_L = \frac{1}{1 + K_L C_0} \tag{4}$$

where C_0 (mg L^{-1}) is the highest initial concentration of adsorbent. The parameter R_L indicates the nature of the isotherm shape to be either favorable ($0 < R_L < 1$), unfavorable ($R_L > 1$), irreversible ($R_L = 0$), or linear ($R_L = 1$) [21].

The Freundlich isotherm is an empirical equation employed to describe heterogeneous systems. The linearized form of the Freundlich model equation is given as:

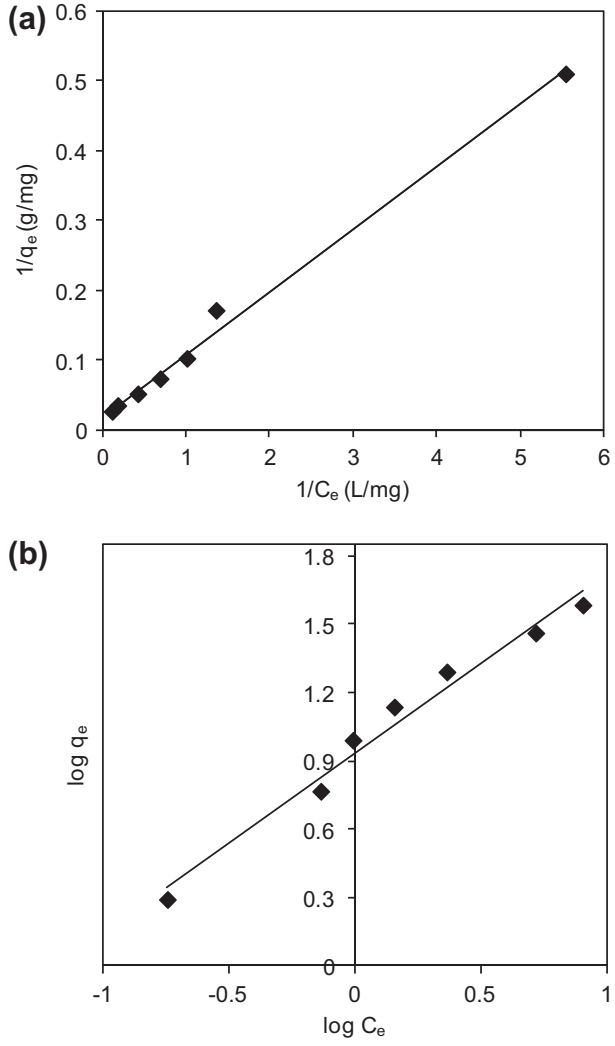

Fig. 7. Langmuir (a) and Freundlich (b) isotherms for the removal of DB 60 by treated DZH.

Table 1
The constants of Langmuir and Freundlich isotherms at 30°C

Adsorption isotherm	Constant
Langmuir	
q_m (mg g^{-1})	54.6
K_L (L mg^{-1})	0.205
R^2	0.994
R_L	0.024
Freundlich	
K_F	8.59
n	1.27
R^2	0.977

$$\log q_e = \frac{1}{n}\log C_e + \log K_F \quad (5)$$

where q_e is the amount of dye adsorbed per unit weight of adsorbent at equilibrium (mg g^{-1}), C_e is the equilibrium concentration of dye in the solution (mg L^{-1}), and K_F and n are the Freundlich adsorption isotherm constants, which indicate the capacity of the adsorbent for the adsorbate and the degree of nonlinearity between the solution concentration and amount adsorbed, respectively. The values of K_F and n can be calculated from the intercept and slope, respectively, of the linear plot between log q_e and log C_e (Fig. 7(b)) and are listed in Table 1.

The value of R_L was 0.024, which indicates that the DB 60 adsorption behavior onto the adsorbent could be considered as favorable with a maximum adsorption capacity (q_{max}) of 54.6 mg g^{-1}. The value n from the Freundlich equation was between 1 and 10 (i.e. $1/n$ was less than 1), which also represents a favorable adsorption [22]. However, it is apparent from both of the R^2 values that the experimental data were best fit to the Langmuir model ($R^2 = 0.999$) rather than the Freundlich model ($R^2 = 0.943$). These results verified that adsorption occurred as the monolayer dyes adsorbed onto the DZH surface. Other researchers have also reported a Langmuir model for the adsorption of disperse dyes [23]. The maximum adsorption capacity of DZH from Langmuir isotherm equation for DB 60 was comparable and was found to be the higher than that of many corresponding adsorbents reported in the literature (Table 2) [23–25].

3.5. Kinetic studies

Kinetic studies are important in dye adsorption to explain the dye uptake rate, the diffusion process and also the mechanism of adsorption, which can imply that the adsorbate either physically or chemically adsorbs onto the surface of the adsorbent [23]. As shown in Fig. 2, the adsorption of 50 mg L^{-1} DB 60 using treated DZH progressed rapidly for the first 15 min to give a removal of 85% and then gradually increased to 98% after 120 min of contact time. Similar patterns of adsorption were observed for six different concentrations ranging from 10–200 mg L^{-1} DB 60 (figure not shown). These results were then used to analyze the kinetics of adsorption using the three most widely used equations: Lagergren's pseudo-first-order model [26], Ho's pseudo-second-order model [27] and Weber and Morris's intraparticle diffusion model [28].

The linearized form of Lagergren's pseudo-first-order model equation is presented as:

Table 2
Adsorption capacities of various adsorbents for disperse dyes

Dyes	Adsorbents	q_{max} (mg/g)	References
Disperse blue	Palm ash	49.5	[29]
Disperse red 60	Bio-sludge	40.0 ± 0.1	[30]
Disperse blue 60	Bio-sludge	31.3 ± 3.8	[30]
Disperse red 1	Bentonite	22.7	[31]
Disperse red 1	Fly ash	30.0	[31]
Disperse red 1	Slag	33.2	[32]
Disperse blue 60	DZH	54.6	This study

Table 3
Adsorption kinetic parameters for the adsorption of DB 60 onto treated DZH at different initial concentrations

Initial conc. (mg/L)	$q_{e,exp}$ (mg/g)	Pseudo-first-order model			Pseudo-second-order model			Intraparticle diffusion		
		k_1 (1/min)	$q_{1e,cal}$ (mg/g)	R^2	k_2 (g/mg min)	$q_{2e,cal}$ (mg/g)	R^2	k_P (mg/g $min^{1/2}$)	C (mg/g)	R^2
10	2.00	0.095	1.87	0.882	0.1509	2.06	0.999	0.340	0.270	0.964
30	5.97	0.071	5.14	0.931	0.0474	6.16	0.999	0.993	0.928	0.987
50	9.46	0.090	8.75	0.875	0.0306	9.78	0.999	1.692	1.404	0.967
70	13.0	0.081	12.16	0.883	0.0183	13.55	0.998	2.450	3.366	0.990
100	18.0	0.059	16.64	0.909	0.0082	19.16	0.993	3.684	7.313	0.997
150	21.0	0.055	18.88	0.926	0.0068	22.37	0.993	4.185	8.039	0.996
200	22.0	0.038	20.80	0.953	0.0025	25.51	0.980	4.192	9.711	0.997

$$\log(q_{1e} - q_t) = \log q_{1e} - \frac{k_1}{2.303} t \quad (6)$$

where k_1 is the rate constant of the pseudo-first-order model [29]. Plotting the log (q_{1e}–q_t) against t should give a straight line (figure not shown), and the value of k_1 can be calculated from its slope (Table 3).

Ho's pseudo-second-order model in linearized form is shown as the following equation,

$$\frac{t}{q_t} = \frac{1}{k_2 q_{2e}^2} + \frac{t}{q_{2e}} \quad (7)$$

where k_2 is the rate constant of the pseudo-second-order model. The value of k_2 can be calculated from the intercept and slope of the linear plot of t/q_t against t (Fig. 8).

The regression coefficients of the second-order model were higher than those of the first-order model for all initial concentrations studied (Table 3), indicating that the experimental data were best fit to the second-order model. The results also demonstrated that the values of theoretically obtained $q_{2e,cal}$ values were closer to the experimental $q_{e,exp}$ values at different initial DB 60 concentrations. Therefore, the pseudo-second-order model, rather than the first-order kinetic model, could better explain the adsorption of DB 60 onto DZH. Similar results have been observed in the adsorption of disperse dyes onto fungal biomass, palm oil ash, and bio-sludge [22–24]. From these observations, the rate of dye adsorption is most likely controlled by a chemisorption process.

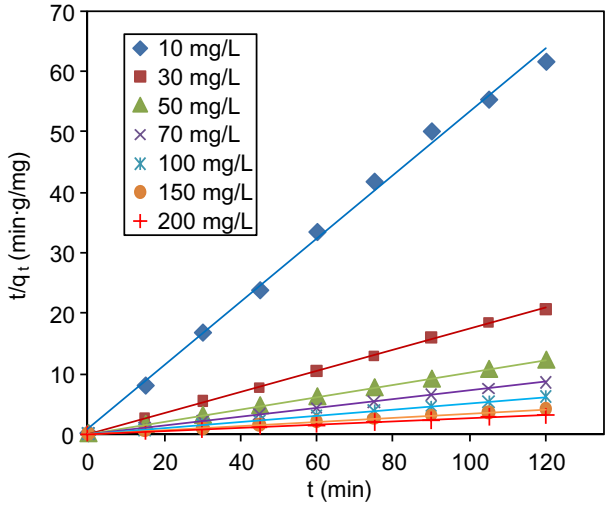

Fig. 8. Pseudo-second-order kinetic plots for DB 60 adsorption onto treated DZH.

The experimental data were then analyzed by using the intraparticle diffusion model (Eq. (8)) to identify the diffusion mechanism of DB 60 onto the surface of DZH.

$$q_t = k_p t^{1/2} + C \tag{8}$$

The variable k_p is the intraparticle diffusion rate constant (mg g^{-1} min$^{-1/2}$) and C is a constant for the measure of the boundary layer thickness (mg g^{-1}), which both value can be evaluated from the slope and intercept of the linear plot of q_t vs. $t^{1/2}$, respectively (Fig. 9). Values of k_p and C, are given in Table 3 for all initial concentrations. If the regression of q_t vs. $t^{1/2}$ is linear and passes through the origin, then intraparticle diffusion is the sole rate-limiting step [29]. However, as shown in Fig. 9, the plots were not linear over the whole time range and instead seemed to be separated into multi-linear curves, indicating that multiple stages were involved in the adsorption process with a rapid diffusion rate in the initial stage at each DB 60 concentrations. The first linear portion represents the fastest step, which corresponds to the diffusion of DB 60 towards DZH. The second line is a delayed process that represents intra-particle diffusion, while the third line represents the diffusion through small pores, which is followed by the establishment of equilibrium [29] due to the saturation of most of the adsorption sites [30]. The large values of C suggest that the process was largely of surface adsorption [31].

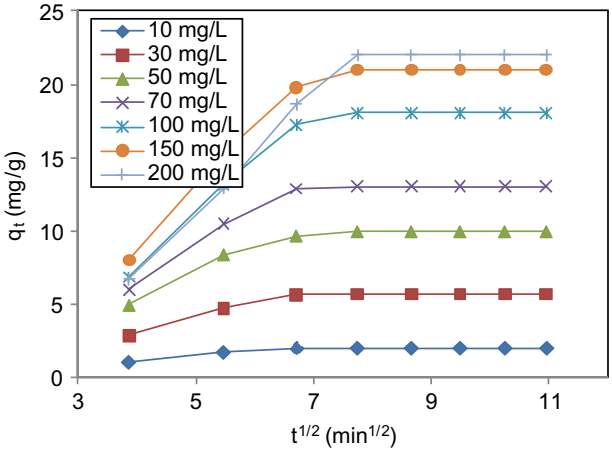

Fig. 9. Intraparticle diffusion plots for the adsorption of DB 60 by treated DZH at 30°C.

3.6. Thermodynamics studies

The effect of temperature on the adsorption rate of DB 60 onto DZH was investigated at three different temperatures (303, 313, and 323 K) using initial concentration of 50 mg L^{-1} DB 60. As shown in Table 4, the adsorption capacity of DB 60 increased as the temperature increased, illustrating that the adsorption process is endothermic in nature. These experimental data were then used to investigate the thermodynamics parameters for the adsorption.

The thermodynamic parameters, such as Gibbs free energy change (ΔG°), standard enthalpy (ΔH°), and standard entropy (ΔS°), can be calculated using the following equations:

$$\Delta G^\circ = -RT\ln K_C \tag{9}$$

$$\ln K_C = -\frac{\Delta H^\circ}{RT} + \frac{\Delta S^\circ}{R} \tag{10}$$

where K_C is the adsorption equilibrium constant, which is obtained from Eq. (11).

$$K_C = \frac{C_{Ae}}{C_{Se}} \tag{11}$$

C_{Ae} is the amount of dye (mg) adsorbed onto the adsorbent per L of solution at equilibrium, and C_{Se} is the equilibrium concentration (mg L^{-1}) of the dye in the solution. Eq. (10) is the so-called Van't Hoff equation and R is the gas constant (8.314 J mol^{-1} K^{-1}). The values of ΔH° (kJ mol^{-1}) and ΔS° (kJ mol^{-1}) were calculated from the slope and intercept, respectively, of the plot ln K_C vs. $1/T$ (Fig. 10), and all of the thermodynamic parameters are listed in Table 4. The positive value of ΔH° signifies the endothermic nature of the process, which confirms the fact that the adsorption efficiency increased with increasing temperatures [29].

Table 4
Values of thermodynamic parameters for removal DB 60 by treated DZH

Temperature (K)	q_e (mg g^{-1})	ΔG (kJ mol^{-1})	ΔH (kJ mol^{-1})	ΔS (kJ mol^{-1} K^{-1})	E_a (kJ mol^{-1})
303	9.80	5.77			
313	15.0	7.47	43.8	0.164	51.5
323	19.7	9.04			

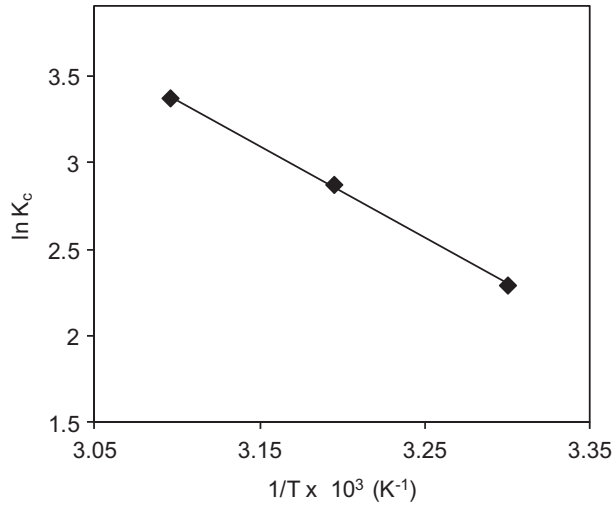

Fig. 10. Plot of ln K_C vs. $1/T$ for estimation of thermodynamic parameters.

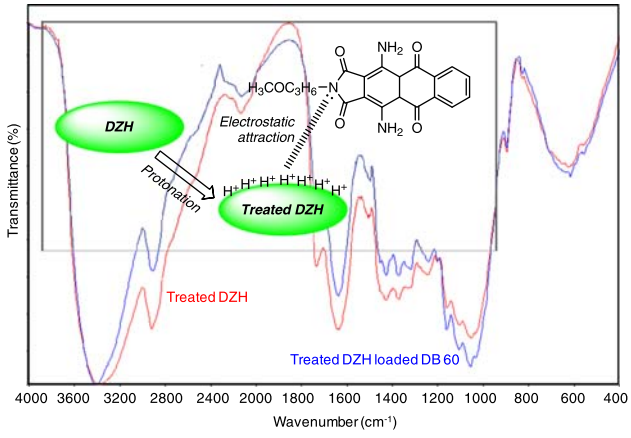

Fig. 11. FTIR spectra of treated DZH loaded DB 60 and the proposed mechanism of the adsorption at 30°C.

It is well known that the magnitude of enthalpy can provide information on the type of adsorption, which can be either physical or chemical. However, there are a number of contradictory cases in the literature. In this study, its magnitude fell into a range of 20.9–418.4 kJ mol^{-1}, giving information that the adsorption of DB 60 onto the DZH surface had taken place via chemisorption processes [32–38]. This observation is in agreement with the fact that the process fit well with the pseudo-second-order kinetic models, verifying the process was controlled by a chemisorption mechanism. In addition, the magnitude of the activation energy may also give the same information about the type of sorption. The activation energy for DB 60 adsorption onto DZH was 51.5 kJ mol^{-1} (Table 4) and was derived from the slope of the Arrhenius plot of ln k_2 vs. $1/T$ (Eq. (12)),

$$\ln k_2 = \ln A - \frac{E_a}{RT} \tag{12}$$

where k_2 is the rate constant value for the pseudo-second-order kinetic model, T is the temperature in Kelvin, and R is the gas constant (8.314 J mol^{-1} K^{-1}). The magnitude of E_a (between 40 and 800 kJ mol^{-1}) also supports the fact that the adsorption process onto DZH was due to chemisorption [22]. The positive value of ΔS° suggested an increasing randomness at the solid–solution interface during the adsorption of DB 60 onto DZH. All positive values of ΔG° obtained in the range of temperatures studied here demonstrated that the adsorption reaction was not spontaneous and that the system gained energy from an external source [29].

3.7. Proposed mechanism of adsorption of DB 60 onto DZH

Fig. 11 shows the proposed mechanism of the DB 60 adsorption onto treated DZH and the FTIR spectra of treated DZH before and after adsorption of the dye. The peaks at 3,416, 2,912, 2,136, 1,731, 1,638,

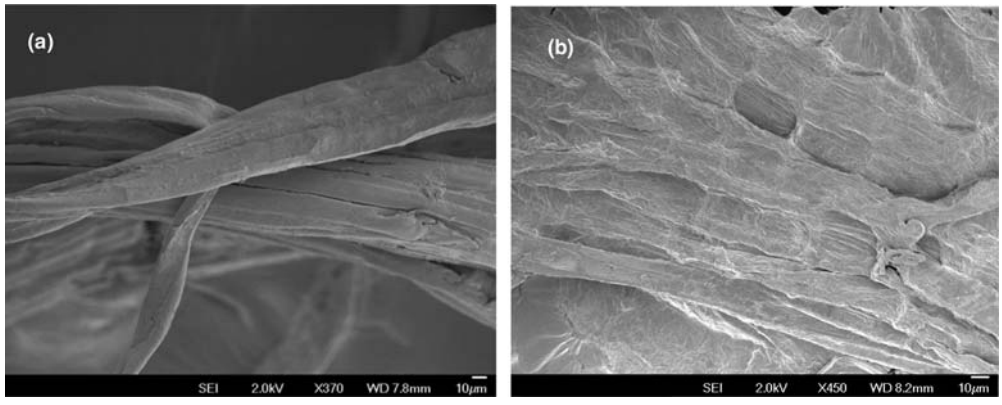

Fig. 12. The FESEM images before (a) and after (b) the adsorption of DB 60 onto treated DZH.

1,428, 1,369, 1,318, and 1,244 cm^{-1}, which may correspond to –OH groups, $–CH_2–$groups, C=N stretching, C=O stretching, C=C group, –OH bending, CH_3 deformation, C–N stretching, and C–O stretching, respectively, were slightly shifted and/or decreased in intensity after adsorption, indicating the possibility of weak electrostatic interaction between the treated DZH and the anionic DB 60 molecules [22,39]. The intensity of the bands observed at 1,162, 1,111, and 1,055 cm^{-1} was slightly increased and shifted to 1,059, 1,106 and 1,049 cm^{-1}. These spectral changes confirmed the possible involvement of amines (C–N) groups of DB 60 with the protonated DZH surface by nucleophilic substitution [12,39].

Textural structure analysis by FESEM before (Fig. 12(a)) and after (Fig. 12(b)) adsorption also indicated that the rough and fibrous surface of the DZH before the adsorption became smoother and stickier due to the packing of the dye.

4. Conclusion

This study showed that HCl-treated DZH acts as a good adsorbent for the removal of DB 60 from aqueous solutions. The amount of the dye adsorbed was found to be dependent on solution pH, contact time, adsorbent dosage, initial DB 60 concentration, and temperature. The DB 60 was almost completely removed from the aqueous solution at optimum conditions of 5 g L^{-1} treated DZH, pH 9, and 30°C after 1 h of contact time. Equilibrium data were best defined by the Langmuir isotherm model, and the kinetic results were fit to the pseudo-second-order model. These results indicate that the treated DZH has potential to be used in dye removal processes from aqueous solutions.

Acknowledgments

Our gratitude goes to Ministry of Higher Education Malaysia for their financial supports under the Fundamental Research Grant. We are also grateful to the Hitachi Scholarship Foundation and Professor Dr Goto Masahiro from Kyushu University, Japan for their supports.

References

[1] D.A. Fungaro, M. Bruno, L.C. Grosche, Adsorption and kinetic studies of methylene blue on zeolite synthesized from fly ash, Desalin. Water Treat. 2 (2009) 231–239.
[2] Z. Aksu, Application of biosorption for the removal of organic pollutants: A review, Process Biochem. 40 (2005) 997–1026.
[3] E.A. Oliveira, S.F. Montanher, M.C. Rollemberg, Removal of textile dyes by sorption on low-cost sobents. A case study: Sorption of reactive dyes onto Luffa cylindrical, Desalin. Water Treat. 25 (2011) 54–64.
[4] K. Turhan, Z. Turgut, Treatment and degradability of direct dyes in textile wastewater by ozonation; A laboratory investigation, Desalin. Water Treat. 11 (2009) 184–191.
[5] J. Khedari, S. Charoenvai, J. Hirumlabh, New insulating particleboards from durian peel and coconut coir, Build. Environ. 38 (2003) 435–441.
[6] M.A.Z. Abidin, A.A. Jalil, S. Triwahyono, S.H. Adam, N.H.N. Kamarudin, Recovery of gold(III) from an aqueous solution onto a *durio zibethinus* husk, Biochem. Eng. J. 54(2) (2010) 124–131.
[7] M.A. Al-Ghouti, J. Li, Y. Salamh, N. Al-Laqtah, G. Walker, M. N.M. Ahmad, Adsorption mechanisms of removing heavy metals and dyes from aqueous solution using date pits solid adsorbent, J. Hazard. Mater. 176 (2010) 510–520.
[8] A.M. Adel, Z.H.A. El–Wahab, A.A. Ibrahim, M.T. Al–Shemy, Characterization of microcrystalline cellulose prepared from lignocellulosic materials. Part I. Acid catalyzed hydrolysis, Bioresour. Technol. 101 (2010) 4446–4455.
[9] A.-N.A. El-Hendawy, Variation in the FTIR spectra of a biomass under impregnation, carbonization and oxidation conditions, J. Anal. Appl. Pyrolysis 75(2) (2006) 159–166.
[10] N.V. Farinella, G.D. Matos, M.A.Z. Arruda, Grape bagasse as a potential biosorbent of metals in effluent treatments, Bioresour. Technol. 98 (2007) 1940–1946.
[11] D. Rosu, C.-A. Teaca, R. Bodirlau, L. Rosu, FTIR and color change of the modified wood as a result of artificial light irradiation, J. Photochem. Photobiol. B: Biol. 99 (2010) 144–149.
[12] T. Akar, M. Divriklioglu, Biosorption applications of modified fungal biomass for decolorization of Reactive Red 2 contaminated solutions: Batch and dynamic flow mode studies, Bioresour. Technol. 101 (2010) 7271–7277.
[13] R. Nadeem, T.M. Ansari, A.M. Khalid, Fourier Transform Infrared Spectroscopic characterization and optimization of Pb(II) biosorption by fish (*Labeo rohita*) scales, J. Hazard. Mater. 156 (2008) 64–73.
[14] A.B. Joshi, L.E. Kirsch, The relative rates of glutamine and asparagine deamidation in glucagon fragment 22–29 under acidic conditions, J. Pharm. Sci. 91(11) (2002) 2331–2345.
[15] Ö. Gerçel, H.F. Gerçel, A.S. Koparal, Ü.B. Öğütveren, Removal of disperse dye from aqueous solution by novel adsorbent prepared from biomass plant material, J. Hazard. Mater. 160 (2008) 668–674.
[16] C.H. Giles, A.P. D'Silva, I.A. Easton, A general treatment and classification of the solute adsorption isotherm Part II. Experimental interpretation, J. Colloid Interface Sci. 47 (1974) 766–778.
[17] D.M. Nevskaia, A. Santianes, V. Muñoz, A. Guerrero-Ruíz, Interaction of aqueous solutions of phenol with commercial activated carbons: An adsorption and kinetic study, Carbon 37(7) (1999) 1065–1074.
[18] I. Langmuir, The adsorption of gases on plane surfaces of glass, mica and platinum, J. Am. Chem. 57 (1918) 1361–1403.
[19] H.M.F. Freundlich, Uber die adsorption in losungen, Z. Phys. Chem. 57 (1906) 385–470.
[20] K.R. Hall, L.C. Eagleton, A. Acrivos, T. Vermeulen, Pore and solid diffusion kinetics in fixed bed adsorption under constant pattern conditions, Ind. Eng. Chem. Fundam. 5 (1966) 212–219.
[21] A.K. Bhattacharya, T.K. Naiya, S.N. Mandal, S.K. Das, Adsorption, kinetics and equilibrium studies on removal of Cr(VI) from aqueous solutions using different low-cost adsorbents, Chem. Eng. J. 137 (2008) 529–541.
[22] A. Tassist, H. Lounici, N. Abdi, N. Mameri, Equilibrium, kinetic and thermodynamic studies on aluminum biosorption by a mycelial biomass (*Streptomyces rimosus*), J. Hazard. Mater. 183 (2010) 35–43.
[23] M.H. Isa, L.S. Lang, F.A.H. Asaari, H.A. Aziz, N.A. Ramli, J. P.A. Dhas, Low cost removal of disperse dyes from aqueous solution using palm ash, Dyes Pigm. 74 (2007) 446–453.

[24] S. Sirianuntapiboon, P. Srisornsak, Removal of disperse dyes from textile wastewater using bio-sludge, Bioresour. Technol. 98 (2007) 1057–1066.
[25] K.R. Ramakrishna, T. Viraraghavan, Use of slag for dye removal, Waste Manage. 17(8) (1997) 483–488.
[26] S. Lagergren, About the theory of so-called adsorption of soluble substances, Kungliga Svenska Vetenskapsakademiens, Handlingar 24 (1898) 1–39.
[27] Y.S. Ho, G. McKay, Pseudo-second order model for sorption processes, Process Biochem. 34 (1999) 451–465.
[28] W.J. Weber, Jr., J.C. Morris, Kinetics of adsorption on carbon from solution, J. Sanit. Eng. Div. Am. Soc. Civ. Eng. 89 (1963) 31–60.
[29] A.A. Jalil, S. Triwahyono, S.H. Adam, N.D. Rahim, M.A.A. Aziz, N.H.H. Hairom, N.A.M. Razali, M.A.Z. Abidin, M.K.A. Mohamadiah, Adsorption of methyl orange from aqueous solution onto calcined Lapindo volcanic mud, J. Hazard. Mater. 181 (2010) 755–762.
[30] L. Abramian, H. El-Rassy, Adsorption kinetics and thermodynamics of azo-dye Orange II onto highly porous titania aerogel, Chem. Eng. J. 150 (2009) 403–410.
[31] O. Aksakal, H. Ucun, Equilibrium, kinetic and thermodynamic studies of the biosorption of textile dye (Reactive Red 195) onto *Pinus sylvestris L*, J. Hazard. Mater. 181 (2010) 666–672.
[32] A. Sari, M. Tuzen, Biosorption of total chromium from aqueous solution by red algae (*Ceramium virgatum*): Equilibrium, kinetic and thermodynamic studies, J. Hazard. Mater. 160 (2008) 349–355.
[33] A. Sari, D. Mendil, M. Tuzen, M. Soylak, Biosorption of Cd (II) and Cr(III) from aqueous solution by moss (*Hylocomium splendens*) biomass: Equilibrium, kinetic and thermodynamic studies, Chem. Eng. J. 144 (2008) 1–9.
[34] R.A. Anayurt, A. Sari, M. Tuzen, Equilibrium, thermodynamic and kinetic studies on biosorption of Pb(II) and Cd(II) from aqueous solution by macrofungus (*Lactarius scrobiculatus*) biomass, Chem. Eng. J. 151 (2009) 255–261.
[35] A. Sarı, M. Tuzen, Kinetic and equilibrium studies of biosorption of Pb(II) and Cd(II) from aqueous solution by macrofungus (*Amanita rubescens*) biomass, J. Hazard. Mater. 164 (2009) 1004–1011.
[36] A. Sarı, M. Tuzen, Removal of mercury(II) from aqueous solution using moss (*Drepanocladus revolvens*) biomass: Equilibrium, thermodynamic and kinetic studies Original Research Article, J. Hazard. Mater. 171 (2009) 500–507.
[37] M. Tuzen, A. Sari, D. Mendil, M. Soylak, Biosorptive removal of mercury(II) from aqueous solution using lichen (*Xanthoparmelia conspersa*) biomass: Kinetic and equilibrium studies, J. Hazard. Mater. 169 (2009) 263–270.
[38] A. Sarı, M. Tuzen, Biosorption of Pb(II) and Cd(II) from aqueous solution using green alga (*Ulva lactuca*) biomass, J. Hazard. Mater. 152 (2008) 302–308.
[39] B.H. Hameed, R.R. Krishni, S.A. Sata, A novel agricultural waste adsorbent for the removal of cationic dye from aqueous solutions, J. Hazard. Mater. 162 (2009) 305–311.